Directed Gas Phase Formation of the Elusive Silylgermylidyne Radical (H_3SiGe, X^2A'')

Zhenghai Yang,[a] Srinivas Doddipatla,[a] Ralf I. Kaiser,*[a] Vladislav S. Krasnoukhov,[b] Valeriy N. Azyazov,[b] and Alexander M. Mebel*[c]

The previously unknown silylgermylidyne radical (H_3SiGe; X^2A'') was prepared via the bimolecular gas phase reaction of ground state silylidyne radicals (SiH; $X^2\Pi$) with germane (GeH_4; X^1A_1) under single collision conditions in crossed molecular beams experiments. This reaction begins with the formation of a van der Waals complex followed by insertion of silylidyne into a germanium-hydrogen bond forming the germylsilyl radical (H_3GeSiH_2). A hydrogen migration isomerizes this intermediate to the silylgermyl radical (H_2GeSiH_3), which undergoes a hydrogen shift to an exotic, hydrogen-bridged germylidynesilane intermediate ($H_3Si(\mu\text{-}H)GeH$); this species emits molecular hydrogen forming the silylgermylidyne radical (H_3SiGe). Our study offers a remarkable glance at the complex reaction dynamics and inherent isomerization processes of the silicon-germanium system, which are quite distinct from those of the isovalent hydrocarbon system (ethyl radical; C_2H_5) eventually affording detailed insights into an exotic chemistry and intriguing chemical bonding of silicon-germanium species at the microscopic level exploiting crossed molecular beams.

1. Introduction

For more than a century, Langmuir's perception of isovalency, in which 'two molecular entities with the same number of valence electrons have similar chemistries'[1] has been instrumental in rationalizing fundamental principles of molecular structure and the reactivity of isovalent systems along with advancing novel synthetic chemistry and modern concepts of chemical bonding.[2] Special devotion has been attributed to comparing the chemistries of main group XIV elements germanium (Ge) and silicon (Si) with the second row analogous carbon (C) chemistry.[3] Although Langmuir's concept envisages that the molecular structure and chemical bonding of isovalent systems should be identical, the actual molecular geometries of isovalent systems involving main group XIV elements may differ remarkably. Therefore, the chemistry of multiple bonded, heavier main group species has prompted extensive interest because of the unusual chemical properties, structures, and often exotic chemical bonding.[4] The existence of double and triple bonds of the heavier main group XIV elements (Si, Ge, Sn, Pb) was doubted for decades prior to the discovery of the stable distannene in 1973[5] and the synthesis of the diplumbyne in 2000.[6] Subsequently, alkyne analogs including distannyne,[7] digermyne[8] and disilyne[9] were prepared. Besides, the isomerization of heavier analogues of ethynes E_2H_2 (E═Si–Pb) to vinylidene-analogs was studied, and stable vinylidene analogs were synthesized.[10] The diverse chemical bonding of carbon versus silicon and germanium is also reflected in a comparison of the homo- (E_2H_3) and heteronuclear ($EE'H_3$) trihydrides, i.e. highly reactive and unstable doublet radicals, with E and E' representing germanium, silicon, and/or carbon (Scheme 1). For the hydrocarbon system, the planar vinyl radical (C_2H_3; **1**; X^2A') has a C_s point group and corresponds to the global minimum of the C_2H_3 potential energy surface (PES),[3a,11] whereas the methylmethylidyne radical (CH_3C; **2**; X^2A'') is thermodynamically less stable by 205 kJ mol^{-1}. Considering the six Si_2H_3 species – among them four hydrogen bridged structures – the thermodynamically most stable Si_2H_3 isomer – the quasi-planar H_2SiSiH molecule (Si_2H_3; **3**; X^2A) does not have any symmetry at all with the hydrogen atoms slightly bent out-of-plane.[3b,12] Similarly, the most stable structure of the Ge_2H_3 system is a vinyl-type radical H_2GeGeH (Ge_2H_3; **9**; X^2A''), but the unpaired electron belongs to a π-type orbital.[3c,13] In analogy to the vinyl (C_2H_3; **1**; X^2A') – methylmethylidyne (CH_3C; **2**; X^2A'') isomer pair,[11b] the silylsilylidyne (SiH_3Si; **4**; X^2A'') and germylgermylidyne (GeH_3Ge; **10**; X^2A'') isomers are higher in energy than their vinyl-type counterparts **3** and **9**.

However, for the heteronuclear systems, the sequence of stability is reversed with methylsilylidyne ($SiCH_3$; **15**; X^2A''), methylgermylidyne ($GeCH_3$; **19**; X^2A''), and silylgermylidyne (H_3SiGe; **23**; X^2A'') representing global minima favored by 42, 103, and 29 kJ mol^{-1} compared to their vinyl-type counterparts **16**, **20**, and **25**, respectively.[14] The distinct chemical bonding can be understood in terms of a reduced overlap of the valence s and p orbitals of the silicon and germanium atoms compared

[a] Dr. Z. Yang, Dr. S. Doddipatla, Prof. Dr. R. I. Kaiser
Department of Chemistry
University of Hawaii
Honolulu, HI, 96822, USA
E-mail: ralfk@hawaii.edu
[b] V. S. Krasnoukhov, Prof. Dr. V. N. Azyazov
Samara National Research University
Samara 443086 and Lebedev Physical Institute
Samara 443011, Russian Federation
[c] Prof. Dr. A. M. Mebel
Department of Chemistry and Biochemistry
Florida International University
Miami, FL 33199, USA
E-mail: mebela@fiu.edu

Supporting information for this article is available on the WWW under https://doi.org/10.1002/cphc.202000913

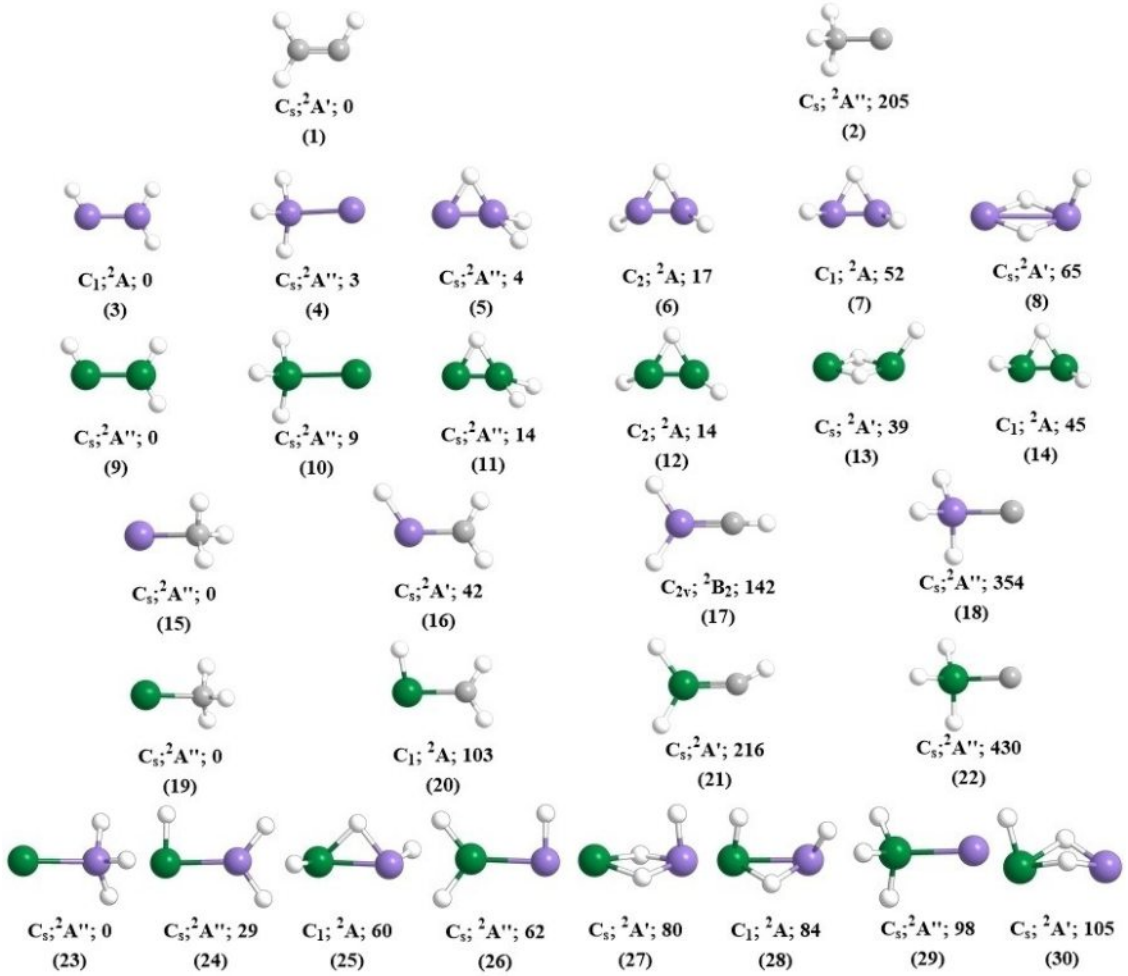

Scheme 1. Structures, point groups, electronic ground state wave functions, and relative energies (kJ mol^{-1}) of homo- and heteronuclear trihydrides of main group XIV elements involving carbon (gray), silicon (purple) and germanium (green) with hydrogen atoms color coded in white.

to carbon.[15] The exotic chemical bonding and unusual molecular structures of silicon and germanium are best reflected considering the non-classical mono- and dibridged $H_2Si(\mu\text{-}H)Si$ (**5**; X^2A''), $HSi(\mu\text{-}H)SiH$ (**6**; X^2A), $HSi(\mu\text{-}H)SiH$ (**7**; X^2A), $HSi(\mu\text{-}H_2)Si$ (**8**; X^2A') and $H_2Ge(\mu\text{-}H)Ge$ (**11**; X^2A''), $HGe(\mu\text{-}H)GeH$ (**12**; X^2A), $HGe(\mu\text{-}H_2)Ge$ (**13**; X^2A'), and $HGe(\mu\text{-}H)GeH$ (**14**; X^2A) isomers, whose carbon analogue structures do not exist. Consequently, the replacement of isovalent carbon by silicon or germanium leads to molecules, whose hydrocarbon counterparts might not represent (local) minima.

Although considerable research has been conducted in understanding the chemical bonding and structures of the homonuclear (C_2H_3, Si_2H_3, Ge_2H_3)[3b,c,11,12c] and heteronuclear systems ($SiCH_3$, $GeCH_3$),[14a,b,16] special attention was attributed to the experimental characterization of hydrogenated silicon-germanium species ($GeSiH_x$). Due to the their technological applications such as chemical vapor deposition,[17] semiconductor processing,[18] silicon-germanium nanowires,[19] germanium-silicon films,[20] and modulation doped field effect transistors (MODFET),[21] the structures, energetics, and spectroscopic properties of silicon-germanium clusters have attracted considerable interest. However, an experimental characterization of *any* $GeSiH_3$ isomer has remained still elusive with only hydrogenated forms ($GeSiH_6$, $GeSiH_5$, $GeSiH_4$) being isolated in the gas phase, liquid state, solid state or in low temperature matrices; recently, the germaniumsilylene butterfly molecule ($Ge(\mu\text{-}H_2)Si$) was prepared via the bimolecular gas phase reaction.[15,20,22] Electronic structure calculations predict the existence of eight structural isomers with silylgermylidyne (H_3SiGe; **23**; X^2A'') representing the global minimum mainly due to the stronger silicon-hydrogen bond compared to the weaker germanium-hydrogen bond.[20] Therefore, the unexplored $GeSiH_3$ system and the silylgermylidyne (H_3SiGe; **23**; X^2A'') radical in particular can be contemplated as a target of a directed gas phase synthesis thus providing fundamental knowledge on the chemical reactivity and unconventional synthetic pathways of highly reactive open shell silicon- and germanium-bearing species.

Here, we report on the very first generation and observation of the hitherto unknown silylgermylidyne (H_3SiGe; **23**; X^2A'') molecule under single-collision conditions in the gas phase through the crossed molecular beam reaction of the silylidyne

radical (SiH; $X^2\Pi$) with germane (GeH_4; X^1A_1). Combining the experimental data with electronic structure calculations, this system can be classified as a benchmark to explore the consequence of a single-collision event between the silylidyne radical transient and the simplest saturated germanium bearing molecule – germane – to initiate silicon-germanium bond coupling eventually forming the silylgermylidyne radical (H_3SiGe; **23**; X^2A''). By generating this species in the gas phase under single collision conditions, the nascent reaction products are formed under experimental conditions without the possibility of successive reactions that prevents secondary processes such as dimerization and cyclo addition thus offering a universal synthetic strategy under controlled experimental conditions to prepare highly reactive transient species.[23] This enables us to synthesize highly reactive species previously not accessible by traditional synthetic chemistry routes and sheds light on the unusual germanium-silicon chemistry, which strongly diverges from those of isovalent carbon-based systems.

2. Methods

2.1. Experimental

The crossed beam experiments of ground state silylidyne radicals (SiH, $X^2\Pi$) with germane (GeH_4; X^1A_1) were carried out under single collision conditions in a crossed molecular beams machine.[23a,24] A pulsed supersonic beam of ground state silylidyne radicals (SiH, $X^2\Pi$) was generated via photolysis of 0.5% disilane (Si_2H_6; 99.998%; Voltaix) seeded in helium (He; 99.9999%; Gaspro) at 193 nm.[25] The pulsed beam of the silylidyne radicals passed through a skimmer and a four-slit chopper wheel rotating at 120 Hz selecting a part of the supersonic beam with a well-defined peak velocity (v_p) and speed ratio (S) of 1744 ± 11 ms^{-1} and 16.7 ± 1.8, respectively. The chopper wheel motor (2057S024B, Faulhaber) was interfaced to a precision motion controller (MC 5005 S RS, Faulhaber). Cables between the motor and the controller had to be shielded to ensure an interference-free operation of the motor. At frequencies of 480 Hz, the 2083.3 μs signal period was stable within ± 0.1 μs as determined via a digital oscilloscope (TDS 2024B, Tektronix). In the interaction region, this section of the pulse intersected the most intense part of a pulsed beam of germane (Air Liquide, 99.999%). The peak velocity and speed ratio of the germane pulse were determined to be 529 ± 5 ms^{-1} and 9.0 ± 0.7 yielding a nominal collision energy of 35.0 ± 0.4 kJ mol^{-1} as well as a center-of-mass (CM) angle of $39.2 \pm 0.2°$. To allow a 'laser-on' minus 'laser-off' background subtraction, both pulsed valves were triggered at 120 Hz, but the laser was operated at half of the repetition rate at 60 Hz. The reactively scattered products were mass filtered after electron impact ionization utilizing a quadrupole mass spectrometer (QMS) operated in the time-of-flight (TOF) mode; ions are monitored by a Daly-type detector housed in a rotatable, triply-differentially pumped ultrahigh vacuum chamber (7×10^{-12} Torr).[26] This complete detector assembly is rotatable within the plane spanned by both supersonic beams to record angular-resolved TOF spectra. To collect information on the scattering dynamics, the laboratory data were transformed from the laboratory into the CM reference frame exploiting a forward-convolution routine[27] yielding an angular flux distribution, $T(\theta)$, and translational energy flux distribution, $P(E_T)$, in the CM system. The laboratory TOF spectra and the angular distributions are then reconstructed from the $P(E_T)$ and $T(\theta)$ functions.[28]

2.2. Computational

Geometries of the reactants, products, intermediates, and transition states partaking in the $SiH + GeH_4$ reaction were optimized with the doubly hybrid DFT B2PLYPD3 method[29] and Dunning's correlation-consistent cc-pVTZ basis set.[30] Vibrational frequencies and zero-point vibrational energy corrections (ZPE) were evaluated at the same B2PLYPD3/cc-pVTZ level of theory. All connections between transition states and local minima were verified by intrinsic reaction coordinate (IRC) calculations. Single-point energies of the optimized structures were rectified using the explicitly correlated coupled clusters CCSD(T)-F12/cc-pVQZ-f12 method[31] to approximate CCSD(T)/CBS energies within the coupled clusters theory with single and double excitations with perturbative treatment of triple excitations in the complete basis set limit. The anticipated accuracy of the CCSD(T)-F12/cc-pVQZ-f12//B2PLYPD3/cc-pVTZ + ZPE (B2PLYPD3/cc-pVTZ) relative energies is typically within 4 kJ mol^{-1}.[32] B2PLYPD3 calculations were performed using the Gaussian 09[33] software package and the CCSD(T)-F12 calculations were carried out using Molpro 2010.[34] Rice-Ramsperger-Kassel-Marcus (RRKM) theory,[35] was used to compute energy-dependent rate constants of all unimolecular reaction steps on the $SiGeH_5$ PES following the initial formation of the **i0** complex in the entrance channel. Internal energy dependent rate constants were computed within the harmonic approximation using B2PLYPD3/cc-pVTZ frequencies using our in-house code,[36] which automatically processes GAUSSIAN 09 log files to assess numbers of states for transition states and densities of states for local minima employing the direct count method. The internal energy was assumed to be equal to the sum of the collision energy and the chemical activation energy, that is, negative of the relative energy of a species with respect to the reactants. Only one energy level was considered throughout as at a zero-pressure limit corresponding to crossed molecular beams conditions. The RRKM-computed rate constants were utilized to obtain product branching ratios by solving first-order kinetic equations within steady-state approximation.[36–37]

3. Results and Discussion

The reactive scattering experiments were performed under single collision conditions at a collision energy of 35.0 ± 0.4 kJ mol^{-1} utilizing a crossed molecular beam apparatus (see the Supporting Information; Table S1).[23a] The neutral reaction

products were ionized at 80 eV via electron impact within a triply differentially pumped quadrupole mass spectrometric (QMS) detector operated at 7×10^{-12} Torr. The ions were then mass-and velocity-analyzed while recording angular resolved time-of-flight (TOF) spectra. Considering the natural isotope abundances of silicon [^{28}Si (92.2%), ^{29}Si (4.7%), ^{30}Si (3.1%)] and of germanium [^{70}Ge (20.4%), ^{72}Ge (27.3%), ^{73}Ge (7.7%), ^{74}Ge (36.7%), ^{76}Ge (7.8%)], reactive scattering signal was probed from mass-to-charge (m/z) of m/z = 110 ($^{76}Ge^{30}SiH_4^+$) to m/z = 98 ($^{70}Ge^{28}Si^+$) with signal at m/z = 102 ($^{74}Ge^{28}Si^+/^{73}Ge^{29}Si^+/^{72}Ge^{30}Si^+/^{73}Ge^{28}SiH^+/^{72}Ge^{29}SiH^+/^{72}Ge^{28}SiH_2^+/^{70}Ge^{30}SiH_2^+/^{70}Ge^{29}SiH_3^+/^{70}Ge^{28}SiH_4^+$) depicting the best signal-to-noise ratio; signal at m/z = 105 ($^{76}Ge^{29}Si^+/^{76}Ge^{28}SiH^+/^{74}Ge^{30}SiH^+/^{74}Ge^{29}SiH_2^+/^{73}Ge^{30}SiH_2^+/^{74}Ge^{28}SiH_3^+/^{73}Ge^{29}SiH_3^+/^{72}Ge^{30}SiH_3^+/^{73}Ge^{28}SiH_4^+/^{72}Ge^{29}SiH_4^+$), at m/z = 104 ($^{76}Ge\ ^{28}Si^+/^{74}Ge^{30}Si^+/^{74}Ge^{29}SiH^+/^{73}Ge^{30}SiH^+/^{74}Ge^{28}SiH_2^+/^{73}Ge^{29}SiH_2^+/^{72}Ge^{30}SiH_2^+/^{73}Ge^{28}SiH_3^+/^{72}Ge^{29}SiH_3^+/^{72}Ge^{28}SiH_4^+/^{70}Ge^{30}SiH_4^+$), and signal at mass-to-charge of m/z = 103 ($^{74}Ge^{29}Si^+/^{73}Ge\ ^{30}Si^+/^{74}Ge^{28}SiH^+/^{73}Ge^{29}SiH^+/^{72}Ge^{30}SiH^+/^{73}Ge^{28}SiH_2^+/^{72}Ge^{29}SiH_2^+/^{72}Ge^{28}SiH_3^+/^{70}Ge^{30}SiH_3^+/^{70}Ge^{29}SiH_4^+$) were collected at levels of 20 ± 2%, 44 ± 2%, and 52 ± 3%, respectively, compared to m/z = 102. No signal was detected at m/z = 110 to 107 suggesting the absence of adducts. It is important to note that the TOF spectra recorded at different mass-to-charge ratios reveal identical patterns after scaling and could be fitted with the same center-of-mass functions as of m/z = 105, indicating the existence of a single channel and all lower masses originate from dissociative ionization in the electron impact ionizer. The only product really formed under our experimental conditions is $SiGeH_3$ (m/z = 105) and that it can partly fragments to $SiGeH_2^+$ (m/z = 104), $SiGeH^+$ (m/z = 103), and $SiGe^+$ (m/z = 102).[38] Most importantly, the dissociative ionization channel in the reaction of SiH with GeH_4 will not influence the reaction dynamics of the experiment. The outcome and the kinetics of the reaction can be predicted and interpreted by the Newton diagram kinematic expression.[39''] However, noting that the fragmentation patterns of hydrogenated, dinuclear silicon-germanium clusters are unknown, we cannot elucidate *per se*, if the atomic and/or hydrogen loss channel is open. Considering the best signal-to-noise ratio, angular resolved TOF spectra were collected at m/z = 102 ($^{28}Si^{74}Ge^+$) revealing a broad laboratory angular distribution spread over 50° within the scattering plane as defined by the silylidyne and germane molecular beams (Figure 1). The broad distribution, which is nearly forward-backward symmetric with respect to the center-of-mass (CM) angle of 39.2 ± 0.2° proposes indirect scattering dynamics through the formation of $^{74}Ge^{28}SiH_5$ complex(es). The appearance of the "second peak" of the TOF spectra in Figure 1b shows the effect of the dynamics of the reaction and the large translational energy release, which results in a large recoil circle.

Considering the natural abundances of the isotopes of silicon and of germanium along with the unknown fragmentation patterns of neutral hydrogen deficient $GeSiH_x$ (x = 1–5) species, it is crucial to carry out electronic structure calculations on the doublet $GeSiH_5$ potential energy surface (PES) (Figures 3 and S1). This approach assists in rationalizing the molecular formulae and the structural isomer(s) of the reaction product(s)

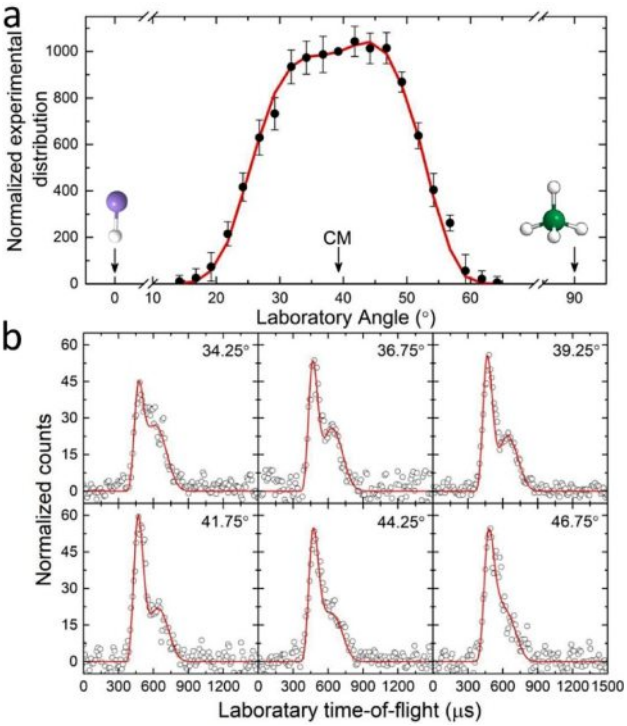

Figure 1. Laboratory angular distribution and associated time-of-flight spectra. Laboratory angular distribution at mass-to-charge ratio (m/z) of m/z = 102 recorded in the reaction of the silylidyne radical with germane (a), and the time-of-flight spectra recorded at distinct laboratory angles overlaid with the best fits (b). The solid circles with their error bars represent the normalized experimental distribution with ±1σ uncertainty; the open circles indicate the experimental data points of the time-of-flight spectra. The red lines represent the best fits obtained from the optimized center-of-mass (CM) functions, as depicted in Figure 2. Silicon, germanium, and hydrogen are color coded in purple, green, and white, respectively.

along with the underlying reaction mechanism governing their formation.[39a] The electronic structure calculations reveal that even the formation of the thermodynamically most stable $GeSiH_4$ isomer silylgermylene (H_3SiGeH; X^1A') formed via atomic hydrogen loss – is endoergic by 63 ± 4 kJ mol^{-1}. Considering the experimental collision energy of 35.0 ± 0.4 kJmol^{-1}, we can therefore conclude that the atomic hydrogen loss channel leading to *any* $GeSiH_4$ isomer is closed under our experimental conditions. As a matter of fact, the laboratory data could be replicated with a single channel fit with the mass combination of the products of 105 amu ($^{74}Ge^{28}SiH_3$; hereafter: $GeSiH_3$) and 2 amu (H_2) with ion counts at m/z = 102 arising from dissociative electron impact ionization of the $^{74}Ge^{28}SiH_3$ parent molecule in the ionizer.

Figure 2 shows the best fit center-of-mass (CM) translational energy $P(E_T)$ and angular flux $T(\theta)$ distributions along with the error limits. The analysis of the CM translational distribution $P(E_T)$ reveals the nature of the product isomer(s). For those reaction products formed without internal excitation, the maximum translational energy, E_{max}, represents the sum of the reaction exoergicity plus the collision energy. For the silylidyne – germane system, a subtraction of the collision energy (35.0 ± 0.4 kJ mol^{-1}) from the maximum translational energy (106 ±

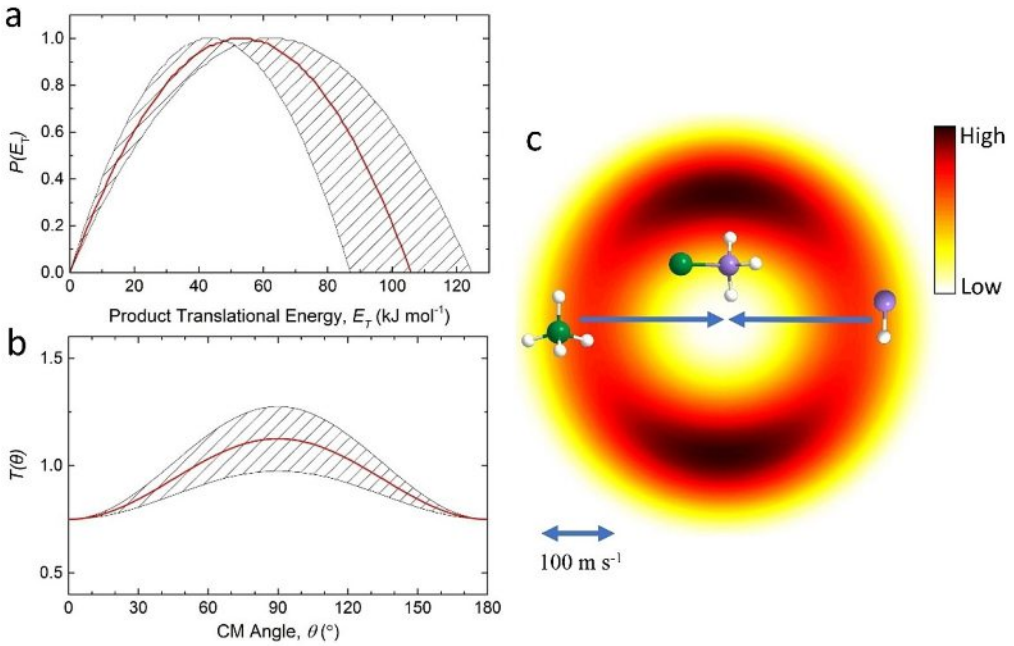

Figure 2. Center-of-Mass (CM) distributions and the associated flux contour map. CM translational energy flux distribution (a), CM angular flux distribution (b), and the top view of their corresponding flux contour map (c) leading to the formation of H_3SiGe plus molecular hydrogen in the reaction of silylidyne with germane. Shaded areas indicate the error limits of the best fits accounting for the uncertainties of the laboratory angular distribution and TOF spectra; the red solid lines define the best-fit functions. The flux contour map represents the flux intensity of the reactive scattering products as a function of the CM scattering angle (θ) and product velocity (u). The color bar indicates the flux gradient from high intensity to low intensity. Silicon, germanium, and hydrogen are color coded in purple, green, and white, respectively.

19 kJ mol^{-1}) reveals that the formation of $GeSiH_3$ along with molecular hydrogen is exoergic by 71 ± 19 kJ mol^{-1}. Further, the distribution maximum of the center-of-mass translational energy distribution of 48 ± 10 kJ mol^{-1} suggests a tight exit transition state and significant electron rearrangement when the intermediate decomposes to the separated products. Further, the center-of-mass (CM) angular flux T(θ) distribution supports indirect (complex forming) reaction mechanisms via unimolecular decomposition of $GeSiH_5$ intermediates since this distribution depicts intensity over the complete scattering range. The forward-backward symmetry proposes that the lifetime(s) of the decomposing reaction intermediate(s) is longer than the(ir) rotational periods, which is larger than 10^{-12} s.[28c,39b] The angular distribution of reactions that proceed through a compound mechanism and where the complex is long living (compared to a rotational period of the interparticle axis) will have a forward-backward symmetry. The dynamics appears to have 'forgotten' the initial direction (long lived complex), the complex only 'remembers' that the angular momentum and energy is conserved. Finally, under our experimental conditions, rotational cooling due to supersonic expansion largely reduces rotational angular momentum *j* of the reactant and thus the total angular momentum *J* lies perpendicular to the relative velocity vector *v*.[39b] When the collision complex is formed, angular momentum dictates that the complex rotates around the(ir) principle axis(xes). In some cases, the complex rotates in the molecular plane perpendicularly to *J*. How this complex decomposes will ultimately determine the shape of the product angular distribution. In our experiment, a dissociation occurs parallel to *J*, the molecular hydrogen is emitted perpendicular (78.6 degrees; Figure 3) to the plane of the rotating $SiGeH_5$ complex and the products are emitted perpendicularly to this plane almost parallel to the total angular momentum vector.[39a,40] So, in Figure 2b, the *T(θ)* displays a maximum at 90°, revealing geometrical constraints in the exit channel with the molecular hydrogen emitted nearly perpendicularly to the rotational plane of the fragmenting intermediate almost parallel to the total angular momentum vector.[39]

The ultimate goal of our study is not only to determine the chemical formula of the reaction product ($GeSiH_3$), but also to elucidate the nature of the isomer formed and the underlying reaction mechanism(s). This is achieved by merging the experimental data with electronic structure calculations (Figure 3). Our electronic structure calculations identified the existence of eight $GeSiH_3$ isomers, which can be prepared via molecular hydrogen loss (**p1**–**p8**). Since the formation of any $GeSiH_4$ isomer via atomic hydrogen loss is closed, these pathways are compiled in the Supplementary Information (Figure S1). The $GeSiH_3$ isomer(s) energetically accessible via the elementary reaction of ground state silylidyne radical (SiH; $X^2\Pi$) with germane (GeH_4; X^1A_1) can be discovered by comparing the experimentally determined reaction energy (-71 ± 19 kJ mol^{-1}) with the reaction energies obtained from our electronic structure calculations for distinct $GeSiH_3$ isomers (Figure 3). This analysis suggests that at least the thermodynamically most stable silylgermylidyne radical (**p1**, H_3SiGe, X^2A'') ($\Delta_R G = -83 \pm$

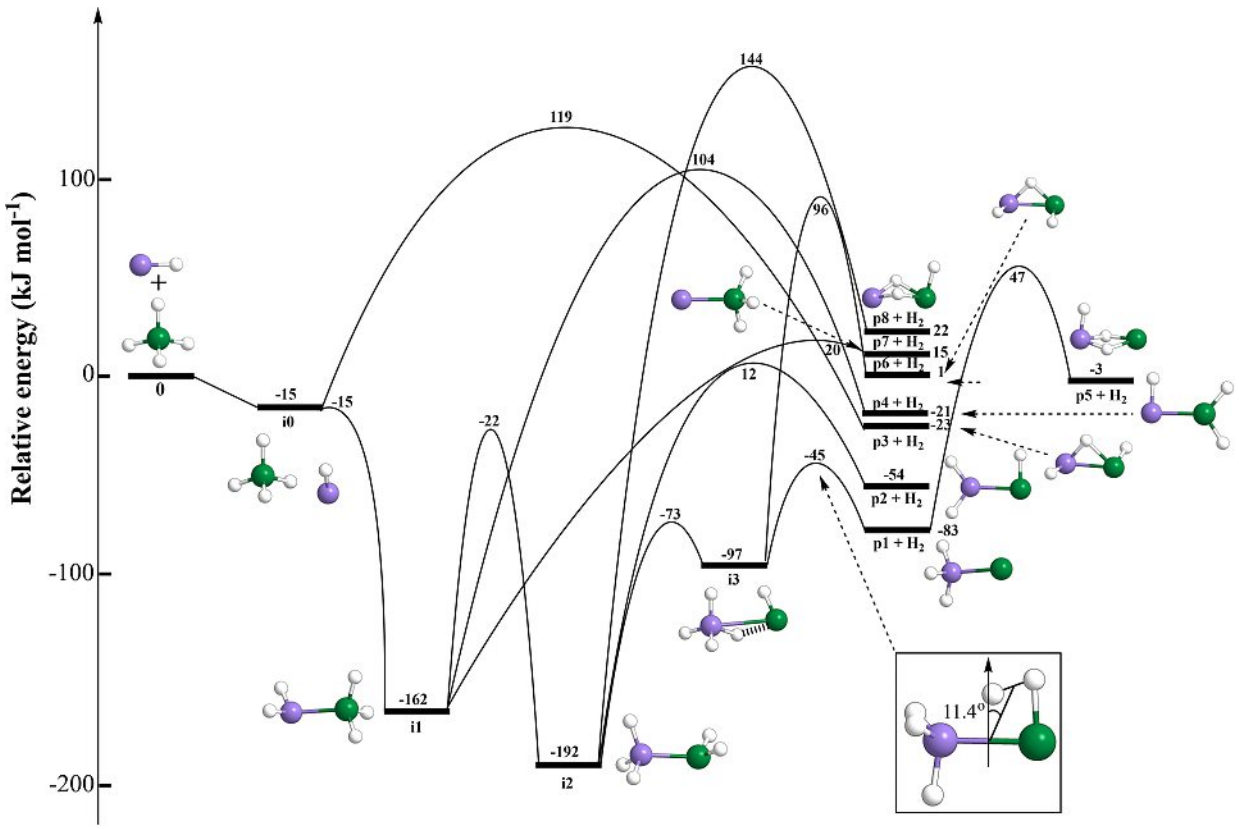

Figure 3. Potential energy surface for the reaction of the silylidyne radical with germane involving molecular hydrogen loss pathways (the insert shows the exit transition state). A complete potential energy surface including the atomic hydrogen loss pathways is presented in Figure S1. Silicon, germanium, and hydrogen are color coded in purple, green, and white, respectively. Optimized Cartesian coordinates and vibrational frequencies are compiled in Table S3.

4 kJ mol^{-1}) and within the error limits possibly silylenegermene (**p2**, $HGeSiH_2$, X^2A'') ($\Delta_R G = -54 \pm 4$ kJ mol^{-1}) is formed. Considering our collision energy of 35.0 ± 0.4 kJ mol^{-1}, the higher energy isomers **p3**–**p8** might represent minor contributors masked in the low energy section of the center-of-mass translational energy distribution. Hence, we can conclude that at least silylgermylidyne (**p1**) and/or silylenegermene (**p2**) represent product(s) of the bimolecular reaction of the silylidyne radical with germane.

With the identification of silylgermylidyne (H_3SiGe, **p1**) and/or silylenegermene ($HGeSiH_2$, **p2**), we would like to reveal now the underlying reaction mechanism(s) to their formation. Our computations suggest that the reaction commences with the formation of a weakly bound van-der-Waals complex **i0**, which is stabilized by only 15 kJ mol^{-1} with respect to the separated reactants. This complex is only metastable and isomerizes via a de-facto barrierless insertion of the silylidyne radical into one of the chemically equivalent germanium-hydrogen single bonds leading to the germylsilyl radical (H_3GeSiH_2, **i1**, X^2A'). Our computations also identified a molecular hydrogen loss from **i0** to the mono-bridged isomer **p3**, but the inherent barrier of 119 kJ mol^{-1} cannot be overcome at our collision energy of 35.0 ± 0.4 kJ mol^{-1}. Intermediate **i1** can then isomerize via a hydrogen shift from the germanium atom to the silicon atom yielding the silylgermyl intermediate (H_2GeSiH_3, **i2**, X^2A') via barrier of 140 kJ mol^{-1}. The silylgermyl radical represents the global minimum of the $GeSiH_5$ PES. Intermediate **i1** could also undergo unimolecular decomposition to **p4** or **p7** plus molecular hydrogen; the barrier from **i1** to **p4** of 104 kJ mol^{-1} cannot be passed at our collision energy; formation of **p7** is endoergic by 15 kJ mol^{-1} and hence contributed less than 13 ± 4% – if at all – of the scattering signal based on the integration of the center-of-mass translational energy distribution from 0 to 20 kJ mol^{-1}. What is the fate of the silylgermyl intermediate (H_2GeSiH_3, **i2**, X^2A')? The molecular hydrogen loss to **p8** is closed by an insurmountable transition state located 144 kJ mol^{-1} above the separated reactants. The formation of silylenegermene ($HGeSiH_2$, **p2**) along with molecular hydrogen is energetically feasible since the overall reaction is exoergic and the exit transition state of 12 kJ mol^{-1} can be overcome at our experimental conditions. However, our computations identified an energetically more favorable pathway via isomerization of **i2** to **i3** followed by molecular hydrogen loss to silylgermylidyne (H_3SiGe, **p1**). The barrier of isomerization and the tight transition state for the molecular hydrogen loss range 85 and 57 kJ mol^{-1} below the transition state connecting **i2** to **p2** plus molecular hydrogen. Therefore, the sequence **i2**→**i3**→**p1** + H_2 is likely favorable. Intermediate **i3** essentially represents a complex between germylidyne and silane with one of the hydrogen atoms of silane located in a bridging position between silicon

and germanium, where the Si–H bond is slightly elongated to 1.535 Å as compared to regular Si–H bonds of 1.47–1.48 Å; the Ge–H distance of 1.89 Å is much longer than normal Ge–H bonds of 1.52–1.53 Å. The Ge–Si distance, 3.01 Å, is also more than 0.5 Å longer than a typical Ge–Si bond, e.g., 2.45 Å in **p1**. When **p1** forms from **i3**, one hydrogen atom is lost from the bridging position and the second hydrogen from the germylidyne (GeH) fragment producing a C_s-symmetric silylgermylidyne radical (**p1**, H_3SiGe, X^2A''), where one of the Si–H bonds (1.492 Å) is slightly distinct from the other two (1.486 Å). The bare germanium atom bears a lone pair in the Ge–Si–H mirror plane and the unpaired electron on a p-orbital perpendicular to this plane (X^2A''). It is interesting to note that the computed geometry of the tight exit transition state **i3**→**p1** + H_2 reveals molecular hydrogen departing nearly parallel to the total angular momentum vector as predicted based on our experimental findings (Figure 3). These conclusions are fully supported by our Rice-Ramsperger-Kassel-Marcus (RRKM) treatment of this system (Supporting Information) revealing – within the limit of a complete energy randomization – fractions of **p1** and **p2** of 99.91% and 0.09%, i.e. a nearly exclusive formation of silylgermylidyne (H_3SiGe, **p1**).

4. Conclusions

In conclusion, our study revealed the first generation and detection of the silylgermylidyne radical (**p1**, H_3SiGe, X^2A'') via the bimolecular gas phase reaction of ground state silylidyne radicals (SiH; $X^2\Pi$) with germane (GeH_4; X^1A_1). The reaction involves indirect scattering dynamics and is initiated by the formation of a van-der-Waals complex, which isomerizes via insertion of silylidyne into a germanium – hydrogen bond yielding the germylsilyl radical (H_3GeSiH_2, **i1**, X^2A'). A successive hydrogen migration transforms this complex to the silylgermyl intermediate (H_2GeSiH_3, **i2**, X^2A'). The later isomerizes via a hydrogen shift to a hydrogen-bridged germylidynesilane intermediate ($H_3Si(\mu\text{-}H)GeH$, **i3**, X^2A), which eventually emits molecular hydrogen via a tight exit transition state yielding the silylgermylidyne radical (**p1**, H_3SiGe, X^2A'') in an overall exoergic reaction (experimental: -71 ± 19 kJ mol^{-1}; computational: -83 ± 4 kJ mol^{-1}).

Despite sharing the same main group XIV, distinct chemical dynamics dictate the outcome of the reactions in the EH–E′H_4 systems (E, E′=C, Si, Ge). While for the methylidyne (CH) – and methane (CH_4) system, the insertion of methylidyne into a carbon-hydrogen bond of methane is also barrierless leading to an ethyl radical intermediate (C_2H_5, X^2A'), which is isovalent to both the germylsilyl (H_3GeSiH_2, **i1**, X^2A') and the silylgermyl radical (GeH_2SiH_3, **i2**, X^2A'), unimolecular decomposition of the ethyl radical intermediate yields the ethylene molecule (C_2H_4; X^1A_{1g}) through atomic hydrogen loss via a tight exit transition state; the molecular hydrogen loss is not accessible.[41] These dynamics are quite distinct from the silylidyne (SiH; $X^2\Pi$) – germane (GeH_4; X^1A_1) system as revealed here illustrating that the isovalency of carbon with silicon and germanium predicts an incorrect reactivity in this system. Consequently, the reactivity of 'heavier' main group XIV atoms isovalent to carbon is difficult to contemplate, and detailed dynamics studies accompanied by electron structure calculations represent the method of choice to untangle the largely unexplored chemical dynamics leading to silicon and germanium-bearing dinuclear analogues of their hydrocarbon counterparts. The comparison of the chemical reactivity of silicon and germanium relative to carbon is fundamental to our understanding of the chemistry of simple hydrides and will influence how we rationalize chemical bonding involving non-classical (hydrogen bridged) transients under single collision conditions. This approach will ultimately expose the similarities, but also unique reactivities of silicon and germanium along with the formation of novel silicon-germanium molecules to gain a comprehensive understanding of their electronic structures, chemical bonding, and stability.

Acknowledgements

The experimental work was supported by the U.S. National Science Foundation (NSF) under Award CHE-1853541. V.S.K. thanks the Ministry of Higher Education and Science of the Russian Federation for his Presidential Scholarship to stay at Florida International University (FIU) in the Spring Semester 2020.

Conflict of Interest

The authors declare no conflict of interest.

Keywords: gas-phase reactions · germane · reaction dynamics · silicon-germanium bond · silylidyne

[1] I. Langmuir, *J. Am. Chem. Soc.* **1919**, *41*, 868–934.
[2] I. Langmuir, *J. Am. Chem. Soc.* **1919**, *41*, 1543–1559.
[3] a) I. M. Nielsen, C. L. Janssen, N. A. Burton, H. F. Schaefer III, *J. Phys. Chem.* **1992**, *96*, 2490–2494; b) L. Sari, M. McCarthy, H. F. Schaefer, P. Thaddeus, *J. Am. Chem. Soc.* **2003**, *125*, 11409–11417; c) W. Carrier, W. Zheng, Y. Osamura, R. I. Kaiser, *Chem. Phys.* **2006**, *330*, 275–286.
[4] R. C. Fischer, P. P. Power, *Chem. Rev.* **2010**, *110*, 3877–3923.
[5] P. J. Davidson, M. F. Lappert, *J. Chem. Soc. Chem. Commun.* **1973**, 317.
[6] L. Pu, B. Twamley, P. P. Power, *J. Am. Chem. Soc.* **2000**, *122*, 3524–3525.
[7] A. D. Phillips, R. J. Wright, M. M. Olmstead, P. P. Power, *J. Am. Chem. Soc.* **2002**, *124*, 5930–5931.
[8] a) M. Stender, A. D. Phillips, R. J. Wright, P. P. Power, *Angew. Chem. Int. Ed.* **2002**, *41*, 1785–1787; b) Y. Sugiyama, T. Sasamori, Y. Hosoi, Y. Furukawa, N. Takagi, S. Nagase, N. Tokitoh, *J. Am. Chem. Soc.* **2006**, *128*, 1023–1031.
[9] a) A. Sekiguchi, R. Kinjo, M. Ichinohe, *Science* **2004**, *305*, 1755–1757; b) A. Sekiguchi, *Pure Appl. Chem.* **2008**, *80*, 447–457.
[10] a) A. Rit, J. Campos, H. Niu, S. Aldridge, *Nat. Chem.* **2016**, *8*, 1022–1026; b) A. Jana, V. Huch, D. Scheschkewitz, *Angew. Chem. Int. Ed.* **2013**, *52*, 12179–12182; c) P. Ghana, M. I. Arz, U. Das, G. Schnakenburg, A. C. Filippou, *Angew. Chem.* **2015**, *127*, 10118–10123.
[11] a) J.-H. Wang, H.-C. Chang, Y.-T. Chen, *Chem. Phys.* **1996**, *206*, 43–56; b) C. J. Bennett, C. S. Jamieson, Y. Osamura, R. I. Kaiser, *Astrophys. J.* **2006**, *653*, 792.
[12] a) D. Sillars, C. J. Bennett, Y. Osamura, R. I. Kaiser, *Chem. Phys. Lett.* **2004**, *392*, 541–548; b) H. Choukri, A. Guermoune, A. R. Schmitzer, D. Villemin, D. Cherqaoui, A. Jarid, *J. Mol. Struct.* **2008**, *852*, 30–35; c) C. Pak, J. C. Rienstra-Kiracofe, H. F. Schaefer, *J. Phys. Chem. A* **2000**, *104*, 11232–11242; d) T. Yang, B. B. Dangi, R. I. Kaiser, K. H. Chao, B. J. Sun, A. H.

Chang, T. L. Nguyen, J. F. Stanton, *Angew. Chem. Int. Ed.* **2017**, *56*, 1264–1268.
[13] a) Q. S. Li, R. H. Lü, Y. Xie, H. F. Schaefer III, *J. Comput. Chem.* **2002**, *23*, 1642–1655; b) A. Ricca, C. W. Bauschlicher, *J. Phys. Chem. A* **1999**, *103*, 11121–11125.
[14] a) Z. Yang, S. Doddipatla, C. He, V. S. Krasnoukhov, V. N. Azyazov, A. M. Mebel, R. I. Kaiser, *Chem. Eur. J.* **2020**, *26*, 13584–13589; b) R. I. Kaiser, Y. Osamura, *Astrophys. J.* **2005**, *630*, 1217; c) G. Trinquier, J. C. Barthelat, J. Satge, *J. Am. Chem. Soc.* **1982**, *104*, 5931–5936.
[15] A. M. Thomas, B. B. Dangi, T. Yang, G. Tarczay, R. I. Kaiser, B.-J. Sun, S.-Y. Chen, A. H. Chang, T. L. Nguyen, J. F. Stanton, *J. Phys. Chem. Lett.* **2019**, *10*, 1264–1271.
[16] a) Z. Yang, C. He, S. Doddipatla, V. S. Krasnoukhov, V. N. Azyazov, A. M. Mebel, R. I. Kaiser, *ChemPhysChem* **2020**, *21*, 1898–1904; b) R. I. Kaiser, W. Carrier, Y. Osamura, R. M. Mahfouz, *Chem. Phys. Lett.* **2010**, *492*, 226–234.
[17] W. B. de Boer, D. J. Meyer, *Appl. Phys. Lett.* **1991**, *58*, 1286–1288.
[18] K. Washio, *IEEE Trans. Electron Devices* **2003**, *50*, 656–668.
[19] G. Chen, G. Springholz, W. Jantsch, F. Schäffler, *Appl. Phys. Lett.* **2011**, *99*, 043103.
[20] A. E. Tomosada, S. Kim, Y. Osamura, S. W. Yang, A. H. Chang, R. I. Kaiser, *Chem. Phys.* **2012**, *409*, 49–60.
[21] K. Ismail, B. Meyerson, P. Wang, *Appl. Phys. Lett.* **1991**, *58*, 2117–2119.
[22] a) S. Mohan, A. Prabakaran, F. Payami, *J. Raman Spectrosc.* **1989**, *20*, 119–121; b) E. J. Spanier, A. G. MacDiarmid, *Inorg. Chem.* **1963**, *2*, 215–216; c) J. Lannon, G. Weiss, E. Nixon, *Spectrochim. Acta Part A* **1970**, *26*, 221–233; d) F. Lampe, *Spectrochim. Acta Part A* **1987**, *43*, 257–264; e) R. Becerra, S. E. Boganov, M. P. Egorov, V. I. Faustov, O. M. Nefedov, R. Walsh, *Phys. Chem. Chem. Phys.* **2001**, *3*, 184–192.
[23] a) R. I. Kaiser, P. Maksyutenko, C. Ennis, F. Zhang, X. Gu, S. P. Krishtal, A. M. Mebel, O. Kostko, M. Ahmed, *Faraday Discuss.* **2010**, *147*, 429–478; b) A. M. Mebel, R. I. Kaiser, *Int. Rev. Phys. Chem.* **2015**, *34*, 461–514.
[24] a) X. Gu, Y. Guo, F. Zhang, A. M. Mebel, R. I. Kaiser, *Faraday Discuss.* **2006**, *133*, 245–275; b) Y. Guo, X. Gu, E. Kawamura, R. I. Kaiser, *Rev. Sci. Instrum.* **2006**, *77*, 034701; c) F. Stahl, P. von Ragué Schleyer, H. Bettinger, R. Kaiser, Y. Lee, H. Schaefer III, *J. Chem. Phys.* **2001**, *114*, 3476–3487; d) R. Kaiser, C. Chiong, O. Asvany, Y. Lee, F. Stahl, P. von R Schleyer, H. Schaefer III, *J. Chem. Phys.* **2001**, *114*, 3488–3496; e) R. Kaiser, A. Mebel, Y. Lee, *J. Chem. Phys.* **2001**, *114*, 231–239.
[25] T. Yang, B. B. Dangi, R. I. Kaiser, L. W. Bertels, M. Head-Gordon, *J. Phys. Chem. A* **2016**, *120*, 4872–4883.
[26] a) N. Daly, *Rev. Sci. Instrum.* **1960**, *31*, 264–267; b) G. O. Brink, *Rev. Sci. Instrum.* **1966**, *37*, 857–860.
[27] a) P. Weiss, *Lawrence Berkeley Lab., CA (USA)* **1986**; b) R. I. Kaiser, T. N. Le, T. L. Nguyen, A. M. Mebel, N. Balucani, Y. T. Lee, F. Stahl, P. v R Schleyer, H. F. Schaefer Iii, *Faraday Discuss.* **2002**, *119*, 51–66.
[28] a) R. D. Levine, *Bull. Chem. Soc. Jpn.* **1988**, *61*, 29–38; b) R. Kaiser, D. Parker, F. Zhang, A. Landera, V. Kislov, A. Mebel, *J. Phys. Chem. A* **2012**, *116*, 4248–4258; c) R. D. Levine, *Molecular Reaction Dynamics*, Cambridge University Press, Cambridge, **2005**.
[29] a) S. Grimme, *J. Chem. Phys.* **2006**, *124*, 034108; b) L. Goerigk, S. Grimme, *J. Chem. Theory Comput.* **2011**, *7*, 291–309; c) S. Grimme, S. Ehrlich, L. Goerigk, *J. Comput. Chem.* **2011**, *32*, 1456–1465.
[30] T. H. Dunning Jr, *J. Chem. Phys.* **1989**, *90*, 1007–1023.
[31] a) T. B. Adler, G. Knizia, H.-J. Werner, *J. Chem. Phys.* **2007**, *127*, 221106; b) G. Knizia, T. B. Adler, H.-J. Werner, *J. Chem. Phys.* **2009**, *130*, 054104.
[32] J. Zhang, E. F. Valeev, *J. Chem. Theory Comput.* **2012**, *8*, 3175–3186.
[33] M. Frisch, G. Trucks, H. Schlegel, G. Scuseria, M. Robb, J. Cheeseman, G. Scalmani, V. Barone, B. Mennucci, *Gaussian 09 Revision D. 01*, Gaussian, Inc.: Wallingford CT, **2009**.
[34] H.-J. Werner, P. Knowles, R. Lindh, F. Manby, M. Schütz, P. Celani, T. Korona, A. Mitrushenkov, G. Rauhut, *MOLPRO, version 2010.1, a package of ab initio programs*, University of Cardiff, Cardiff, UK, **2010**.
[35] a) P. J. Robinson, K. A. Holbrook, *Unimolecular reactions*, Wiley, New York, **1972**; b) H. Eyring, S. H. Lin, S. M. Lin, *Basic chemical kinetics*, John Wiley & Sons, New York, **1980**; c) J. I. Steinfeld, J. S. Francisco, W. L. Hase, *Chemical kinetics and dynamics, Vol. 3*, Prentice Hall, Englewood Cliffs, **1982**.
[36] C. He, L. Zhao, A. M. Thomas, A. N. Morozov, A. M. Mebel, R. I. Kaiser, *J. Phys. Chem. A* **2019**, *123*, 5446–5462.
[37] V. Kislov, T. Nguyen, A. Mebel, S. Lin, S. Smith, *J. Chem. Phys.* **2004**, *120*, 7008–7017.
[38] a) R. I. Kaiser, *Chem. Rev.* **2002**, *102*, 1309–1358; b) R. I. Kaiser, N. Balucani, *Acc. Chem. Res.* **2001**, *34*, 699–706; c) R. Kaiser, H. Lee, A. Mebel, Y. Lee, *Astrophys. J.* **2001**, *548*, 852–860.
[39] a) R. D. Levine, *Molecular reaction dynamics*, Cambridge University Press, Cambridge, UK, **2009**; b) W. Miller, S. Safron, D. Herschbach, *Discuss. Faraday Soc.* **1967**, *44*, 108–122.
[40] a) R. Kaiser, Y. Lee, A. Suits, *J. Chem. Phys.* **1996**, *105*, 8705–8720; b) R. Grice, *Int. Rev. Phys. Chem.* **1995**, *14*, 315–326; c) K. Liu, *J. Chem. Phys.* **2006**, *125*, 132307.
[41] a) P. Fleurat-Lessard, J.-C. Rayez, A. Bergeat, J.-C. Loison, *Chem. Phys.* **2002**, *279*, 87–99; b) A. Canosa, I. R. Sims, D. Travers, I. W. Smith, B. Rowe, *Astron. Astrophys.* **1997**, *323*, 644–651; c) J. M. Ribeiro, A. M. Mebel, *Mol. Phys.* **2015**, *113*, 1865–1872.

Manuscript received: November 4, 2020
Revised manuscript received: November 25, 2020
Accepted manuscript online: November 27, 2020
Version of record online: December 16, 2020